STUDY OF SUM OF COMPLEX EXPONENTIAL SIGNALS

STUDY OF SUM OF COMPLEX EXPONENTIAL SIGNALS

BY

CHENYUJING (ECHO) WANG, B.Eng.

A THESIS

SUBMITTED TO THE DEPARTMENT OF ELECTRICAL & COMPUTER ENGINEERING

AND THE SCHOOL OF GRADUATE STUDIES

OF MCMASTER UNIVERSITY

IN PARTIAL FULFILMENT OF THE REQUIREMENTS

FOR THE DEGREE OF

MASTER OF APPLIED SCIENCE

Master of Applied Science (2020) McMaster University

(Electrical & Computer Engineering) Hamilton, Ontario, Canada

TITLE:	Study of Sum of Complex Exponential Signals
AUTHOR:	Chenyujing (Echo) Wang B.Eng. (Electrical Engineering), McMaster University, Hamilton, Canada
SUPERVISOR:	Dr. Jian-Kang Zhang
NUMBER OF PAGES:	x, 59

Abstract

This thesis focuses mainly on a finite sum of complex exponential signals. This kind of signal model usually captures a variety of applications involving damped signals such as magnetic resonance spectroscopy, gravitational wave bursts, synchronized neuronal hyppocampal rhythms, financial modelling and the acoustic localization of underground oil field. Each coefficient and complex exponential function in the sum signal can be uniquely characterized by the z-transform of the sampling signal of the continuous-time sum signal as its poles and residues. We study the estimation of all these parameters using Pade approximation theory. The Pade approximation theory deals primarily with the optimally asymptotic approximation of a rational fraction with each of the denominator and numerator having an allowable degree to the z-transform of a given discrete-time signal. The poles and the residues of the rational fraction normally provide relatively precise information on the poles and the residues of the original z-transform. Particularly for the sum of complex exponential signals, its poles and the residues can be completely characterized by its Pade approximation rational fraction with a proper degree constraint. Hence, the Pade approximation theory becomes a very strong mathematical tool for studying such sum of complex exponential signals. We make two kinds of contributions: (a) When the residues are all equal to each other, we derive a closed-form formula for determining the

Pade approximation rational fraction as well as for predicting the future data points. (b) A co-prime sampling scheme is proposed, with a closed-form algorithm being provided for efficiently determining the original poles and residues using elementary diophantine theory.

TO MY FAMILY AND MY LOVE

Acknowledgements

First of all, I would like to express my sincerest and deepest gratitude to my supervisor Dr. Jian-Kang Zhang from Department of Electrical and Computer Engineering, McMaster University, not only for his initial and ongoing support for this thesis, but also for his patient, knowledgeable, helpful and consistent supervision throughout my whole program. I would not have completed this work successfully without his support and guidance.

Last but not least, I would like to thank Dr. Dongmei Zhao, Dr. Xiaolin Wu and Dr. Jun Chen for being members of my defence committee. I appreciate their time for reviewing my thesis and providing valuable feedback.

Contents

List of Figures

List of Tables

Chapter 1

Introduction and Problem Statement

1.1 Introduction

With the rapid growth of scientists, investors, companies, or even strategists of countries to rely on data analysis to make decisions according to their needs, it is vital to choose the most efficient mathematical model that can help extract the features of their data. More and more inquiries suggest that the needs of an efficient and accurate prediction method that can apply to any remote devices such as cell phones, tablets, or laptops are essential.

Padé approximation has been widely used in many fields for data analysis, mainly aiming to help involve the cases with damped data, sharp signals, or data with complicated time dependence using its advantages of the time-consuming and shorter period needed. In general, we conclude all those cases as finite sum of complex exponential

signals. For damped data, the involving applications like magnetic resonance spectroscopy (Belkic and Belkic, 2006) that uses the concept of Fast Fourier Transform in the field of life and health, customarily used for biochemical tests, especially the presence of tumors. In the underground oil field, the method can help locate where the sound is transmitted from, and to determine the data transmission of a right path and its position in three-dimensional space, such as measuring-while-drilling (Perotti and Wojtylak, 2018). In the mechanical field, it is applicable for early detection to find pipe leaks of water distribution (Hunaidi and Chu, 1999) and helicopter shafts, and so on (Perotti and Wojtylak, 2018). On the other hand, Padé approximation gets involved in the Finance industry for financial modeling (Junior and Franca, 2011), such as price expectation and finding the ratios of stock market indices with damped oscillations (Wu, 2014).

In this thesis, we can find the unique poles of padé approximants when the padé approximation is represented in matrix form with exact degree of m and n. The distribution of unique poles represents one of the data features. Similarly, an alternative way of finding poles of nth Padé approximant is the generalized eigenvalue problem

$$\tilde{\mathbf{H}}\mathbf{v} = \lambda\mathbf{H}\mathbf{v}$$

At this point, $\mathbf{H}$ is a Hankel matrix, and $\tilde{\mathbf{H}}$ is the corresponding shifted Hankel matrix. The idea of this method is from (B. Beckermann and Labahn, 2007). The generalized Eigenvalue problem occurs in numbers of applications such as the reconstructions to shape a polygon from its moments (Gene H. Golub and Varah, 1999); in algebra, it helps to find a sparse black box's hidden powers (Mark Giesbrecht and shin Lee, 2009) and even for the stated problem, which is the poles of Padé approximants.

Unlike the traditional padé approximation, we will not emphasize the problem on how to use Padé algorithm for data approximation. Our work's main contribution is that we have proposed a competitive prediction model by using the features of data extracted from padé approximation to predict for more related simulation data. Philosophically speaking, our approach is one of the mathematical models that rely upon the features of simulation data generated initially from padé approximation for data prediction. Once we achieve results on current tasks, considerately, we will move on to the prediction model implementation on simulation data with noise and real-world training data. Due to convenience in configuration, our resemble model can be further developed as an off-the-shelf application that can be downloaded on any remote devices to address the related problems effectively and accurately to help more target audiences in various fields.

On the other hand, we propose a theory of co-prime sampling, which is one of our main technical contributions to this thesis that can efficiently determine the original poles and residues of the sum signal. We also provide detailed proof of the argument and the simulation data groups within implementations, where the simulation data have similar features of the sum signals.

1.2 Thesis's structure

At the beginning of the thesis, it states the reasons and motivations of this thesis. Then the following chapter 2 will successively review the general padé approximation, which is categorized into two parts, the background, and theory related features in exact-degree matrix form. Moreover, the alternative method, which is the generalized problem of Hankel matrices, is shown in this chapter. Next, chapter 3 introduces our

proposed prediction algorithm based on padé approximation, followed by our own built simulation data and their implementations. We also compare the simulation output versus the prediction results after implementations.

Furthermore, the next chapter introduces the co-prime sampling theory. We prove this theory and show groups of simulation data with implementations. Eventually, We conclude our work and discuss our plans on potential enhancement and application of the prediction algorithm based on padé approximation.

Chapter 2

Background and Related Work

In this section, we shall briefly discuss the well-known Padé approximation (Nicholas Daras, 2011) and the relations when Padé approximation theory with exact degree m and n in Exact Arithmetic form. In addition to that, we will demonstrate how to find the poles of Padé approximants and its alternative method, the generalized eigenvalue problem.

2.1 General Padé approximation theory

Let $f(z)$ be an analytic function around $z = 0$ with Taylor series:

$$f(z) = \sum_{k=0}^{\infty} c_k z^k \tag{2.1.1}$$

Alternatively, f could be a formal power series. Given a non-negative integer $n \geq 0$,

let $P_n[z]$ denote the set of polynomials of degree at most m, and given another non-negative $m \geq 0$, let $R_{mn}[z]$ be a set of rational functions that can be written as $\frac{p(z)}{q(z)}$ with $p(z) \in P_m[z]$ and $q(z) \in P_n[z]$, or we call it Padé approximant to function f when r_{mn} whose Taylor series is equal to zero. It was initially suggested by Froissart (Froissart, 1969), and now we should recognize poles of Padé approximants *Froissart doublets.*

2.2 Padé approximation with exact degree m&n

According to the general theory of Padé approximation, $f(z) = c_0 + c_1 z + c_2 z^2 + ...$ is a function in a neighborhood of z = 0 with Taylor series. We consider its vector of coefficients $c_k := (c_0,\ c_1,\ c_2 \dots)$. As mentioned above, let P_n denote the set of polynomials of degree at most n, and, given $m \geq 0$ and $n \geq 0$, let R_{mn} be the set of a rational function of $p(z)/q(z)$, or Padé approximants of type(m, n). Throughout the whole thesis, assuming the relationship of degree is $m = n - 1$. If $\mu \leq m$ and $\nu \leq n$ such that $r \in R_{\mu\nu}$, then we say that r is of exact type(μ, ν) had and $\delta = min\{m-\mu, n-\nu\} \geq= 0$ as to R_{mn}. Based on the first chapter of (Pedro Gonnet and Trefethen, 2018), the Padé approximant to $f(z)$ is when the difference of $r_{mn} \in R_{mn}$ and its function f of Taylor series at $z = 0$ compares with function f:

$$r_{mn}(z) - f(z) = \mathcal{O}(z^{maximum}) \tag{2.2.1}$$

From (G. A. Baker and Graves-Morris, 1996), we know that the rational function r_{mn} is unique. The above is a nonlinear equation, in order to get a linear relationship,

multiplying (2.2.1) by the denominator $q(z)$ of r_{mn} to get series at $z = 0$ is

$$p(z) = \mathcal{O}(z^{maximum}) + f(z)q(z) \tag{2.2.2}$$

However, to get to this point, we lack preconditions since it only could be achieved by taking $p(z)$ and $q(z)$ as zero. In order to make itself meaningful, it has to satisfy that $q(z) \neq 0$. With the requirement, we can only write the equation with degree m and n as

$$p(z) = \mathcal{O}(z^{m+n+1}) + f(z)q(z) \tag{2.2.3}$$

Assume $p(z)$ and $q(z)$ satisfy all the preconditions for equation (2.2.3). Suppose $\mathbf{a}$ is a size of $(m + 1)$ vector, it is also the set of coefficients of polynomials $p(z) \in P_m$. Similarly, $\mathbf{b}$ is an $(n + 1)$ vector containing all the coefficients of the denominator $q(z) \in p_n$, which respectively are

$$\mathbf{a} = \begin{bmatrix} a_0 \\ a_1 \\ \vdots \\ a_m \end{bmatrix} \qquad \mathbf{b} = \begin{bmatrix} b_0 \\ b_1 \\ \vdots \\ b_n \end{bmatrix} \tag{2.2.4}$$

$$p(z) = \sum_{l=0}^{m} a_l z^l \qquad q(z) = \sum_{l=0}^{n} b_l z^l$$

Since the conditions of $m = n - 1$, $m \leq n$. The equations of vectors $p(z)$ and $q(z)$ can be represented in matrix form. Normally each coefficient is normalized such as $b_0 = 1$, where might cause the linear system of (2.2.3) to be singular. In order to avoid this problem, we need to satisfy the normalization condition (Pedro Gonnet and Trefethen, 2011) that $\|\mathbf{b}\| = 1$, where$\|.\|$ is the vector 2-norm. The matrix displays

$$\left[\begin{array}{c} a_0 \\ a_1 \\ \vdots \\ a_m \\ \hline a_n \\ a_{n+1} \\ \vdots \\ a_{m+n} \end{array}\right] = \left[\begin{array}{ccccc} c_0 & & & & \\ c_1 & c_0 & & & \\ \vdots & \vdots & \ddots & & \\ c_m & c_{m-1} & \dots & c_0 & \\ \hline c_n & c_m & \dots & c_1 & c_0 \\ c_{n+1} & c_n & c_m & \dots & c_1 \\ \vdots & \vdots & \ddots & & \vdots \\ c_{m+n} & c_{2m} & c_{2m-1} & \dots & c_m \end{array}\right] \left[\begin{array}{c} b_0 \\ b_1 \\ b_2 \\ \vdots \\ b_n \end{array}\right] \tag{2.2.5}$$

Based on the vector $\mathbf{a}$ and $\mathbf{b}$ from (2.2.4), it indicates that $a_n = a_{n+1} = ... = a_{m+n} = 0$, where $\mathbf{a}$ is obtained by multiplying matrix $\mathbf{C}$ which above the line; therefore, the matrix below the line should be null. Since $m = n - 1$, let us separate the matrix into two parts, where the $n \times (n + 1)$ upper matrix above the line called matrix $\mathbf{C}$,

and any entries with an index that less than zero will be null.

$$\mathbf{C} = \begin{bmatrix} c_0 & & & & \\ c_1 & c_0 & & & \\ c_2 & c_1 & c_0 & & \\ \vdots & \vdots & \ddots & & \vdots \\ c_m & c_{m-1} & \dots & c_0 & \end{bmatrix} \tag{2.2.6}$$

Correspondingly, the lower matrix below the line named $\tilde{\mathbf{C}}$, which is a Toeplitz matrix with the same size as upper matrix $\mathbf{C}$.

$$\tilde{\mathbf{C}} = \begin{bmatrix} c_n & c_m & \dots & c_1 & c_0 \\ c_{n+1} & c_n & c_m & \dots & c_1 \\ \vdots & \vdots & \ddots & & \vdots \\ c_{m+n} & c_{2m} & c_{2m-1} & \dots & c_m \end{bmatrix} \tag{2.2.7}$$

Accordingly, $\mathbf{b}$ will be a product of the null vector if multiplying a and $\tilde{\mathbf{C}}$. Since $\tilde{\mathbf{C}}$ is a non-convertible matrix, it always has a non-trivial null vector if we ignore all the other trivial vectors that we can confirm the linear relationship.

$$\tilde{\mathbf{C}}\mathbf{b} = \mathbf{0} \tag{2.2.8}$$

In details:

$$\begin{bmatrix} c_n & c_m & \dots & c_1 & c_0 \\ c_{n+1} & c_n & c_m & \dots & c_1 \\ \vdots & \vdots & \ddots & & \vdots \\ c_{m+n} & c_{2m} & c_{2m-1} & \dots & c_m \end{bmatrix} \begin{bmatrix} b_0 \\ b_1 \\ b_2 \\ \vdots \\ b_n \end{bmatrix} = \mathbf{0}$$

The product of upper matrix $\mathbf{C}$ and vector $\mathbf{b}$ will become vector $\mathbf{a}$, where $\mathbf{b}$ is a non-null vector. The equation takes the form:

$$\mathbf{Cb} = \mathbf{a} \tag{2.2.9}$$

In details,

$$\begin{bmatrix} a_0 \\ a_1 \\ \vdots \\ a_m \end{bmatrix} = \begin{bmatrix} c_0 & & & & \\ c_1 & c_0 & & & \\ c_2 & c_1 & c_0 & & \\ \vdots & \vdots & \ddots & & \vdots \\ c_m & c_{m-1} & \dots & c_0 & \end{bmatrix} \begin{bmatrix} b_0 \\ b_1 \\ b_2 \\ \vdots \\ b_n \end{bmatrix}$$

Padé approximation solves this linear equation if the determinant of a matrix is nonzero. Otherwise it cannot be solved. To get the roots of denominator $q(z)$, we shall use Singular Values Decomposition, SVD (Robert M. Corless and Watt, 1995) of matrix $\tilde{\mathbf{C}}$, a factorization to find the nonzero vector $\mathbf{b}$, in which defines the coefficients of $q(z)$.

$$\tilde{\mathbf{C}} = \mathbf{U}\mathbf{\Sigma}\mathbf{V}^T \tag{2.2.10}$$

$\mathbf{U}$ is an $n \times n$ square matrix and a unitary whose inverse equals its conjugate transpose (Szabo, 2015). $\mathbf{\Sigma}$ is an $n \times (n+1)$ diagonal matrix with diagonal entries that $\sigma_1 \geq \sigma_2 \geq \sigma_3 \geq \cdots \geq \sigma_n \geq 0$, and $\mathbf{V}$ is an $(n+1) \times (n+1)$ matrix which is a unitary at the same time. We also call $\mathbf{\Sigma}$ a matrix of singular values. Suppose in this thesis all the diagonal entries $\sigma_n > 0$, then $\tilde{\mathbf{C}}$ will be rank efficient, which can also lead to $\mathbf{V}$'s final column become the nonzero coefficients of $q(z)$ (Pedro Gonnet and Trefethen, 2018). Let $\hat{\mathbf{C}}$ denote the $n \times n$ matrix obtained by deleting the first column of $\tilde{\mathbf{C}}$. It is noticeable that matrix $\hat{\mathbf{C}}$ can be flipped horizontally into a Hankel matrix, which we can use its features such as (Beckermann, 2000) to help analyze further problems. The matrix $\hat{\mathbf{C}}$ is

$$\hat{\mathbf{C}} = \begin{bmatrix} c_m & \dots & c_1 & c_0 \\ c_n & c_m & \dots & c_1 \\ \vdots & \ddots & & \vdots \\ c_{2m} & c_{2m-1} & \dots & c_m \end{bmatrix} \tag{2.2.11}$$

According to the paper (Pedro Gonnet and Trefethen, 2018), If matrix $\hat{\mathbf{C}}$ is singular, it only has a determinant of 0, then $b_0 = 0$, which also implies $a_0 = 0$, thus $p(z)$ and $q(z)$ share one common factor. Since we state $\|\mathbf{b}\| = 1$, the defect of $\hat{\mathbf{C}}$'s singularity does not exist. If $\hat{\mathbf{C}}$ is non-singular, then b_0 must be nonzero.

On the other hand, if $\sigma_n = 0$, the matrix $\tilde{\mathbf{C}}$ will be rank-deficient, which we assume its rank of ρ with zero diagonal entries $\sigma_{\rho+1} = \cdots = \sigma_n = 0$. This also infers that $\tilde{\mathbf{C}}$ has a zero vector in its first $n - \rho$ place. Then matrix $\hat{\mathbf{C}}$ must have the rank of ρ or $\rho - 1$, and it is singular due to its 0 determinant. However, this defect can be ignored since it does meet our assumption that all the diagonal entries $\sigma_n > 0$.

In this thesis, we assume that $\sigma_n > 0$, with $m = n - 1$. According to the relationship of $\tilde{\mathbf{C}}$ and $\mathbf{b}$ in (2.2.9), the roots of $\mathbf{b}$ will be the poles of denominator $q(z)$. On the other hand, using equation (2.2.4), the roots of $\mathbf{a}$ will be the poles of $p(z)$. If we remove the common roots of $p(z)$ and $q(z)$, the rest of poles should scatter along the unit circle (Gilewicz and Pindor, 1997) .

2.3 The Alternative Method: Generalized Eigenvalue Problem

Other than the Padé approximation with exact degree m and n, there is an alternative method denoted to find poles of Padé approximants, which is the generalized eigenvalue problem stated as $\tilde{\mathbf{H}}\mathbf{v} = \lambda\mathbf{H}\mathbf{v}$. The problem is stated originally from (B. Beckermann and Labahn, 2007). In this case, $\mathbf{H}$ is a Hankel matrix, $\tilde{\mathbf{H}}$ is the corresponding shifted Hankel matrix, λ is the groups of generalized eigenvalues, and $\mathbf{v}$ is the eigenvector. Additionally, the Hankel matrix is a square matrix in which each ascending skew-diagonal from left to right is constant.

Given a group of numbers $h_0, h_1, \ldots, h_{2n-1}$, to form $n \times n$ matrix $\mathbf{H}$ and its shifted $n \times n$ matrix $\tilde{\mathbf{H}}$ from the generalized eigenvalue problem. For Hankel matrices matrix $\mathbf{H}$

$$\mathbf{H} = \begin{bmatrix} h_0 & h_1 & \ldots & h_{n-1} \\ h_1 & h_2 & \ldots & h_n \\ \vdots & \vdots & \vdots & \vdots \\ h_{n-1} & h_{n-2} & \ldots & h_{2n-2} \end{bmatrix} \tag{2.3.1}$$

and its corresponding shifted matrix $\tilde{\mathbf{H}}$

$$\tilde{\mathbf{H}} = \begin{bmatrix} h_1 & h_2 & \dots & h_n \\ h_2 & h_3 & \dots & h_{n+1} \\ \vdots & \vdots & \vdots & \vdots \\ h_n & h_{n-1} & \dots & h_{2n-1} \end{bmatrix} \tag{2.3.2}$$

In terms of Padé approximation problem with exact degree m and n in which mentioned in the previous section, Generalized Hankel Eigenvalue Problem in application of poles of Padé approximants (G. A. Baker and Graves-Morris, 1996). The implementation of this alternative method uses a size of $2 \times n$ entries of vector $\mathbf{c}$ to form the Hankel matrix $\mathbf{A}$ and its corresponding shifted matrix $\mathbf{B}$

$$\mathbf{A} = \begin{bmatrix} c_0 & c_1 & \dots & c_{n-1} \\ c_1 & c_2 & \dots & c_n \\ \vdots & \vdots & \vdots & \vdots \\ c_{n-1} & c_{n-2} & \dots & c_{2n-2} \end{bmatrix} \tag{2.3.3}$$

$$\mathbf{B} = \begin{bmatrix} c_1 & c_2 & \dots & c_n \\ c_2 & c_3 & \dots & c_{n+1} \\ \vdots & \vdots & \vdots & \vdots \\ c_n & c_{n-1} & \dots & c_{2n-1} \end{bmatrix} \tag{2.3.4}$$

The first row of matrix $\mathbf{A}$ equals the second row of matrix $\mathbf{B}$, and both are in the same descending order. After the formation of two matrices, we need to find their

generalized eigenvalues.

$$\mathbf{Bv} = \lambda \mathbf{Av}$$

The eigenvalues will follow the following equation:

$$det(\mathbf{B} - \lambda \mathbf{A}) = \mathbf{0} \tag{2.3.5}$$

$\mathbf{v}$ is the generalized eigenvector, and λ is called generalized eigenvalue of $\mathbf{A}$ and $\mathbf{B}$. If the entries of matrix $\mathbf{c}$ are complex numbers, the eigenvalues will be complex numbers. Since the size of vector $\mathbf{c}$ is $2 \times n$, it will return a column vector containing the generalized eigenvalues of square matrices $\mathbf{A}$ and $\mathbf{B}$, and the size of eigenvalues should be half of the vector $\mathbf{c}$'s size, which is n. According to the well-known (G. A. Baker and Graves-Morris, 1996) and (Gene H. Golub and Varah, 1999), the result of $det(\mathbf{B} - \lambda \mathbf{A})$ is the denominator $q(z)$ of Padé approximants at infinity of the series $f(z)$. Therefore, the generalized eigenvalues are the estimation of poles of Padé approximants in Padé approximation. Additionally, there is a coordinate-based circle which center is at the coordinate $(0, 0)$ with radius 1. The results of generalized eigenvalues should scatter around this circle on coordinate.

Chapter 3

Data Prediction of Padé Approximation and Its Related Work

Padé theory is well-known as an approximation method for various applications that involve finite sum of complex exponential signals in different fields. We have discussed the background and usage of Padé approximation, and its alternative method of Hankel Generalized Eigenvalue problem in the former chapter. However, Padé theory has not been mentioned in the field of data prediction until today. Unlike any other applications of Padé approximation, our main contribution in this thesis is to propose a mathematical model to predict future data. This model is established based on the features extracted from traditional Padé approximation. We call it Data Prediction of Padé approximation. In this chapter, we will discuss algorithms from our proposed data prediction method rigorously, and then we will demonstrate the simulation data sets and their implementations of our proposed method.

3.1 Algorithms of Proposed Method

Let us consider a finite sum of damped oscillation signals, i.e., complex exponential signals

$$c(t) = \sum_{\ell=1}^{n} r_\ell e^{(-\sigma_\ell + i\Omega_\ell)t}$$

The sample signal $c[k] = c(kT)$ is represented by

$$c[k] = \sum_{\ell=1}^{n} r_\ell e^{(-\sigma_\ell + i\Omega_\ell)kT} = \sum_{\ell=1}^{n} r_\ell z_\ell^k$$

where $z_k = e^{(-\sigma_k + i\Omega_k)T}$. Hence, the z-transform of $c[n]$ is given by

$$\sum_{k=0}^{\infty} c[k] z^k = \sum_{\ell=1}^{n} \frac{r_\ell}{1 - z_\ell z} = \frac{p(z)}{q(z)}$$

Notice that

$$r_\ell = \lim_{z \to z_\ell^{-1}} (1 - z_\ell z) \frac{p(z)}{q(z)} = z_\ell^{-1} \lim_{w \to z_\ell} (w - z_\ell) \frac{p(w^{-1})}{q(w^{-1})}$$

Since

$$\frac{p(w^{-1})}{q(w^{-1})} = \frac{w(a_0 w^{n-1} + a_1 w^{n-2} + \cdots + a_{n-1})}{b_0 w^n + b_1 w^{n-1} + \cdots + b_n}$$

we attain

$$\begin{aligned}\lim_{w\to z_\ell}(w-z_\ell)\frac{p(w^{-1})}{q(w^{-1})} &= \lim_{w\to z_\ell}\frac{w(a_0w^{n-1}+a_1w^{n-2}+\cdots+a_{n-1})}{\frac{b_0w^n+b_1w^{n-1}+\cdots+b_n}{w-z_\ell}} \\ &= \frac{z_\ell(a_0z_\ell^{n-1}+a_1z_\ell^{n-2}+\cdots+a_{n-1})}{nb_0z_\ell^{n-1}+(n-1)b_1z_\ell^{n-2}+\cdots+b_{n-1}}\end{aligned}$$

Hence, we have

$$r_\ell = \frac{a_0z_\ell^{n-1}+a_1z_\ell^{n-2}+\cdots+a_{n-1}}{nb_0z_\ell^{n-1}+(n-1)b_1z_\ell^{n-2}+\cdots+b_{n-1}}$$

for $\ell = 1, 2, \cdots, n$. If $r_\ell = 1$, then, we can obtain $a_i = (n-i)b_i$ for $i = 0, 1, \cdots, n-1$. As from equations (2.2.4), **a** and **b** are two vectors of coefficients for polynomials $p(z)$ and $q(z)$, with the exact degree of m and n, respectively. We also set $m = n-1$ throughout the whole thesis. According to the previous explanation, suppose vector **a** has the linear relationship with vector **a** that

$$a_k = (m-k+1)b_k \tag{3.1.1}$$

$$\text{for } k = 0, 1, ...m$$

According to the Padé approximation in terms of degrees m and n from the prior chapter, the size of vector **c** should be $2 \times n$, which are c_0, c_1, $\ldots c_m$, c_n, $\ldots c_{2n-1}$. Suppose a part of the vector from c_0 to c_n are known, and the first entry of vector **b** is $b_0 = 1$. The rest part of the data is what we are looking forward to finding. To predict the unknown data from c_{m+2} to c_{m+n}, we require the equation (2.2.9) that $\mathbf{Cb} = \mathbf{a}$, the relationship of Upper matrix **C**, vector **b**, and **a**. Based on this

mentioned multiplication equation of upper matrix **C** and **b**, in together with index k from 0 to m that we can conclude

$$a_k = c_k b_0 + c_{k-1} b_1 + ... + c_0 b_k$$

for index

$$k = 0, 1, 2, \ldots m$$

Index of **c** is in descending form multiplied with the ascending index of **b**. It is noticeable that the sum of each **b** and **c**'s indexes is always k. Moreover, with this property adopted, we can simplify the above equation into a summation equation that is

$$a_k = \sum_{l=0}^{k} b_l c_{k-l} \tag{3.1.2}$$

In addition to the relationship (3.1.1) above, the combination shows with scalars m, k, variables b_k and c_{k-l}

$$(m - k + 1) b_k = \sum_{l=0}^{k} b_l c_{k-l}$$

We need to find the vector **b** from b_0 to b_m in the first place, and $b_0 = 1$ known at the beginning. In order to simplify the above equation, we can have the representation of **b** is

$$b_k = -\frac{1}{k} \sum_{l=0}^{k-1} b_l c_{k-l} \tag{3.1.3}$$

$$k = 1, 2, \ldots, m$$

As well as when k equals to n, we can get

$$b_n = -\frac{1}{n}\sum_{l=0}^{n-1} b_l c_{n-l} \tag{3.1.4}$$

All the $\mathbf{b}$ values could be determined at this point. It is the time to predict for the rest of $\mathbf{c}$ values from c_{m+2} to c_{m+n}.

Using the relationship of lower matrix $\tilde{\mathbf{C}}$ and $\mathbf{b}$ (2.2.8), the multiplication of lower matrix $\tilde{\mathbf{C}}$ and $\mathbf{b}$ which equals to null, we can get

$$c_{m+k}b_0 + c_{m+k-1}b_i ... + c_m b_k + c_{m-1}b_{k+1} + ...c_{m+k-n}b_n = 0$$

with index

$$2 \leq k \leq n$$

It is noticeable that the sum of $\mathbf{c}$ and $\mathbf{b}$'s indexes are always $m + k$, and we can simplify this equation to a summation algorithm for data prediction, which is

$$c_{m+k} = -\sum_{l=1}^{n} b_l c_{m+k-l} \tag{3.1.5}$$

with index

$$k = 2, 3, ...n$$

Since we are able to find all the entries vector $\mathbf{b}$ from the previous equation (3.1.4), We can predict the rest of $\mathbf{c}$ from c_{m+2} to c_{m+n} using this prediction algorithm. Above all, this is the model for data prediction using Padé approximation. If $\mathbf{c}$'s index is less than 0, the corresponding entry will become zero. Since we have the condition of $m = n - 1$, no index will be less than zero.

3.2 Simulation Data Sets

In this section, we will use the simulation algorithms to generate two groups of simulation Data sets, which contain the input and output of simulation data in each group. After that, we will exhibit three more simulation data sets generated with similar algorithms. First of all, using the extracted features of data from previous Padé approximation to build the algorithm that generates the first group of simulation data set, where we set $m = 2$, $n = 3$ and the first simulation data algorithm will be

$$c_q = e^{S1\times q} + e^{S2\times q} + e^{S3\times q} \tag{3.2.1}$$

with index

$$q = 0, 1, 2, m, n, ...(m + n)$$

Coefficients are

$$S1 = -0.1 - 2\pi \times 0.3i;$$
$$S2 = -0.05 - 2\pi \times 0.28i;$$
$$S3 = -0.0001 + 2\pi \times 0.2i$$

The simulation input data is from c_0 to c_3, and the rest of c_4 and c_5 are simulation output data. The simulation input data are

c_0	c_1	c_2	c_3
$3.00 + 0.00i$	$-1.489 - 0.844i$	$-2.313 + 1.402i$	$0.252 + 0.575i$

The simulation output data are

c_4	c_5
$1.113 - 2.149i$	$-0.237 - 0.458i$

The second group of simulation data set, where we set $m = 4$, $n = 5$ and the second simulation data algorithm will be

$$c_q = e^{q\times i\times \pi/2} + e^{q\times i\times \pi/3} + e^{q\times i\times \pi/4} + e^{q\times i\times \pi/5} + e^{q\times i\times \pi/6} \tag{3.2.2}$$

where the index is

$$q = 0, 1, 2, m, n, ...(m + n)$$

The simulation input data is from c_0 to c_5; the rest of data c_6 and c_9 are simulation output data that will compare with the prediction data.

The simulation input data are

c_0	c_1	c_2
$5.00 + 0.00i$	$2.882 + 3.661i$	$-0.691 + 3.683i$
c_3	c_4	c_5
$0-2.016+1.658i$	$-1.809 + 0.588i$	$-2.073 - 0.073i$

The simulation output data are

c_6	c_7	c_8	c_9
$-1.809 - 1.588i$	$0.032 - 2.292i$	$1.309 - 0.951i$	$0.516 + 0.119i$

Similarly, we generate other groups of data sets based on features of the first and the second simulation algorithms. For example, in the third simulation group, we set $m = 18$, $n = 19$, and this simulation algorithm is an extended version of the first simulation algorithm, which should contain 14 terms. We also set the values from S_1 to S_{19} as complex numbers. As long as each exponent does not have the same unit circle, the algorithm can generate simulation data. The simulation input data set has the size of 20, while the simulation output data should be 18. Moreover, in the forth group of simulation data, we extend the second simulation algorithm with $m = 18$, $n = 19$, which is

$$c_q = e^{q\times i\times \pi/2} + \cdots + e^{q\times i\times \pi/9} + e^{q\times i\times \pi/11} + e^{q\times i\times \pi/12} + \cdots + e^{q\times i\times \pi/20}$$

Therefore, the fourth group includes 20 input and 18 output simulation data. In the end, we provide a simulation algorithm that combines and extends both the first and second algorithms, with $m = 31$ and $n = 32$. The fifth simulation data group has 33 input simulation data and 31 output simulation data.

In the next step, we will apply all the groups of generated input simulation data into

our proposed prediction model individually, which is in purpose to get the prediction results of the index from $m+2$ to $m+n$ of $\mathbf{c}$ as experimental output. The padé prediction values will compare with the last m computer simulation output generated from the simulation algorithms above to check the accuracy of our proposed prediction model. For the last three simulation data groups, we will only compare their output and prediction data individually in figures at the end of this chapter.

3.3 Implementation Of Simulation Data and Results' Comparisons

In this section, we will demonstrate the data-prediction results using our proposed prediction model of Padé approximation from the previous chapter within simulation input data sets to predict entries from the index of $m+2$ to $m+n$, assuming there is no noise in the environment.

First of all, we will input the first simulation data from c_0 to c_n to predict vector $\mathbf{b}$ within size of 4 using equation (3.1.3) and (3.1.4), $b_1 = 1$ known at the beginning. Vector $\mathbf{b}$ from the first data set is

b_0	b_1	b_2	b_3
$1.00 + 0.00i$	$0.149 + 0.844i$	$-0.811 - 0.575i$	$0.627 + 0.589i$

After gaining the first group of vector $\mathbf{b}$, we can obtain the first group's simulation results from index $m+2$ to $m+n$ of $\mathbf{C}$ using the Padé prediction algorithm (3.1.5).

We name it **r**

r_0	r_1
$1.113 - 2.149i$	$-0.237 - 0.458i$

Similarly, for the second group of simulation input data, we can have the size of $n+1$ vector **b**

b_0	b_1	b_2
$1.00 + 0.00i$	$0.149 + 0.844i$	$-0.811 - 0.575i$
b_3	b_4	b_5
$8.258 - 3.538i$	$-4.067 - 2.274i$	$0.156 + 0.988i$

The prediction results of the second group data set are:

r_0	r_1	r_2	r_3
$-1.809 - 1.588i$	$0.032 - 2.292i$	$1.309 - 0.951i$	$0.516 + 0.119i$

To compare the prediction results versus the actual simulation output data, we will also demonstrate them in figures. The first data set comparison has a size of 2 prediction results and simulation output. The results are shown in $Figure3.1$ at the end of this chapter.

The representation of prediction result interacts with the actual output, which means they are the same. The second set of data has the prediction values comparing with the actual output shown in the $Figure3.2$.

From the $Figure3.2$, we can see that our proposed method's prediction results have the same values as the actual simulation data set. Similarly, for the last three simulation data groups, we implement our input data to the proposed prediction method to get the prediction results, and the prediction results are the same as the actual output simulation data. The comparisons appear in $Figure3.3$, $Figure3.4$ and $Figure3.5$ at the end.

After that, we will validate the output results using the alternative method, the generalized Hankel matrices to check if the generalized eigenvalues of two Hankel matrices, which are built by the simulation input and predicted output could relate to the values of e's exponents in the simulation data algorithms that provided at the beginning. For instance, e's exponents of the first simulation data group are $S1$, $S2$ and $S3$. Similarly, e's exponents of the second simulation group are $i \times \pi/2$, $i \times \pi/3$, $i \times \pi/4$, $i \times \pi/5$ and $i \times \pi/6$. The components of e also apply to the results of the other data groups. In detailed steps, the first group of simulation input comes along with its prediction results that can form vector $\mathbf{c}$ with the size of 6. According to Hankel matrices, the first simulation data set from c_0 to c_5 can form two size of $3 * 3$

Hankel matrices $\mathbf{A}$ and $\mathbf{B}$ as the following format

$$\mathbf{A} = \begin{bmatrix} c_0 & c_1 & c_2 \\ c_1 & c_2 & c_3 \\ c_2 & c_3 & c_4 \end{bmatrix} \tag{3.3.1}$$

$$\mathbf{B} = \begin{bmatrix} c_1 & c_2 & c_3 \\ c_2 & c_3 & c_4 \\ c_3 & c_4 & c_5 \end{bmatrix} \tag{3.3.2}$$

Where the first row of $\mathbf{B}$ is the second row of matrix $\mathbf{A}$. The Hankel matrix is in symmetric form. If there is a same size Toeplitz matrix (Böttcher and Grudsky, 2005), and both the Toeplitz matrix and Hankel matrix have the same eigenvalues, then $\mathbf{H}(m,n) = \mathbf{T}(m,n)\,\mathbf{J}_n$, where $\mathbf{J}$ is an exchange matrix (Mazza and Pestana, 2019). Similarly, applying the above steps to the second group of simulation data that can form two sizes of $5 * 5$ Hankel matrices by using the entries from c_0 to c_9. The 2 Hankel matrices of the second group are:

$$\mathbf{A}_2 = \begin{bmatrix} c_0 & c_1 & c_2 & c_3 & c_4 \\ c_1 & c_2 & c_3 & c_4 & c_5 \\ c_2 & c_3 & c_4 & c_5 & c_6 \\ c_3 & c_4 & c_5 & c_6 & c_7 \\ c_4 & c_5 & c_6 & c_7 & c_8 \end{bmatrix} \tag{3.3.3}$$

$$\mathbf{B}_2 = \begin{bmatrix} c_1 & c_2 & c_3 & c_4 & c_5 \\ c_2 & c_3 & c_4 & c_5 & c_6 \\ c_3 & c_4 & c_5 & c_6 & c_7 \\ c_4 & c_5 & c_6 & c_7 & c_8 \\ c_5 & c_6 & c_7 & c_8 & c_9 \end{bmatrix} \tag{3.3.4}$$

Besides, we also need to find the generated eigenvalues after creating two Hankel matrices for each data set. It is remarkable that the generated eigenvalues of each group also distribute along the unit circle, similar to the distribution of padé approximants' poles. This validation process can apply to the rest of the simulation data sets, and the consequences are the same. On the other hand, it is essential to note that each group's generalized eigenvalues should be equal to the exponential of all the exponents, which are respectively from their simulation data algorithms, as we mentioned at the beginning of this section. The generalized eigenvalues of the first simulation data group should be e^{S1}, e^{S2} and e^{S3}. The generalized eigenvalues of the second simulation data group should be $e^{i\times\pi/2}$, $e^{i\times\pi/3}$, $e^{i\times\pi/4}$, $e^{i\times\pi/5}$ and $e^{i\times\pi/6}$. Similar consequences apply to the rest of the simulation data groups.

Overall, both ways show that the prediction method of Padé approximation can be used accurately with simulation datasets without error.

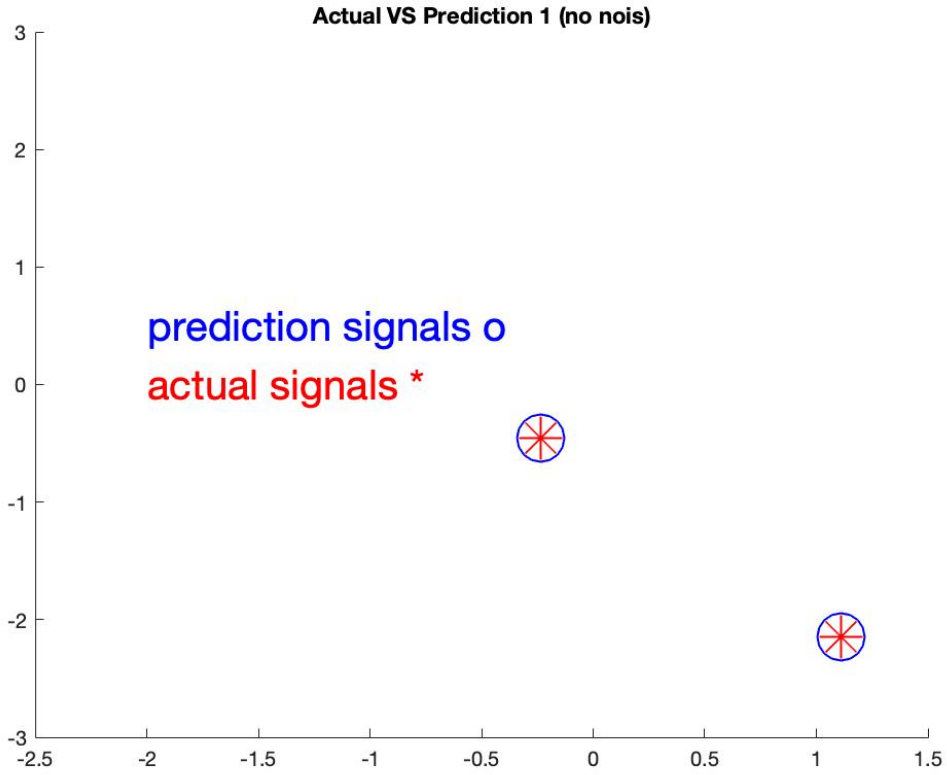

Figure 3.1: First Group: prediction values VS Actual output

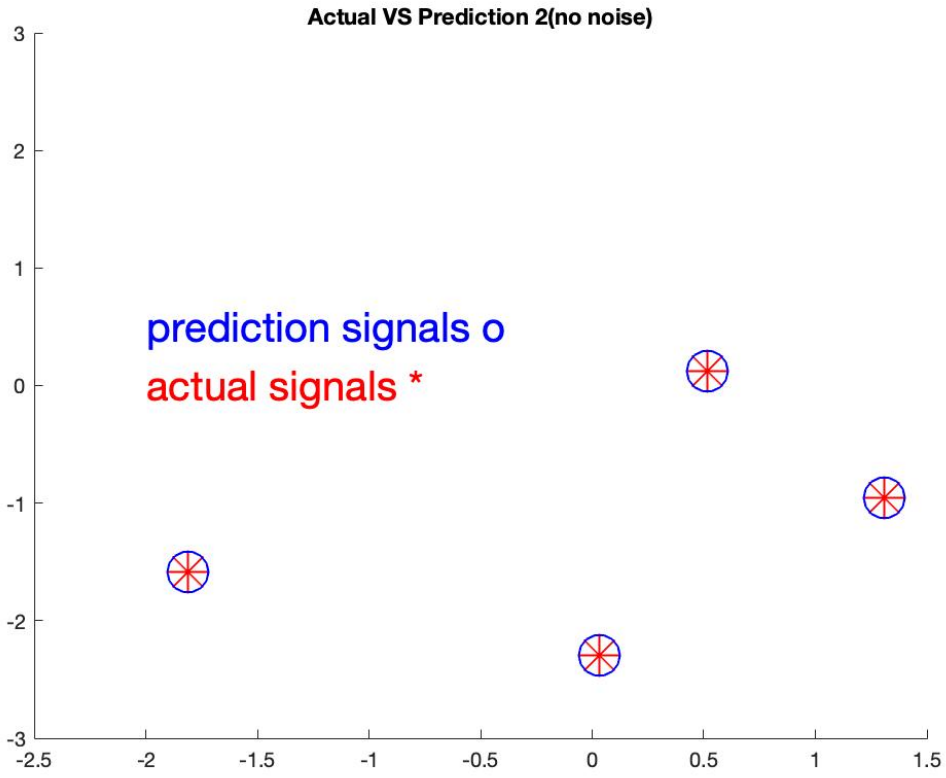

Figure 3.2: Second Group: prediction values VS Actual output

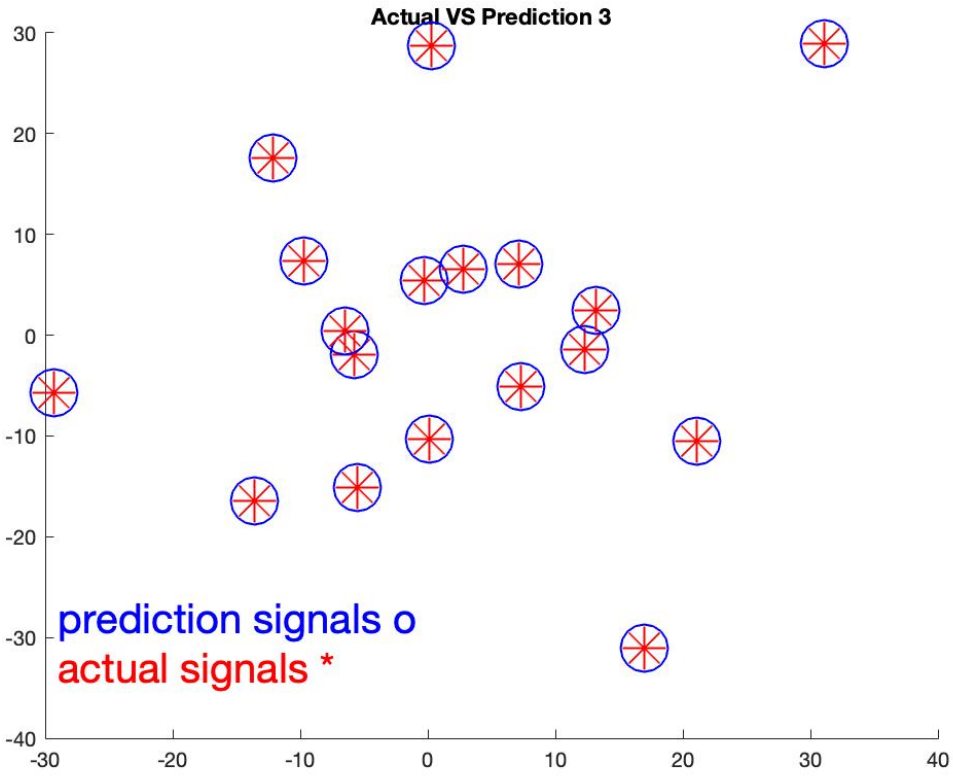

Figure 3.3: Third Group: prediction values VS Actual output

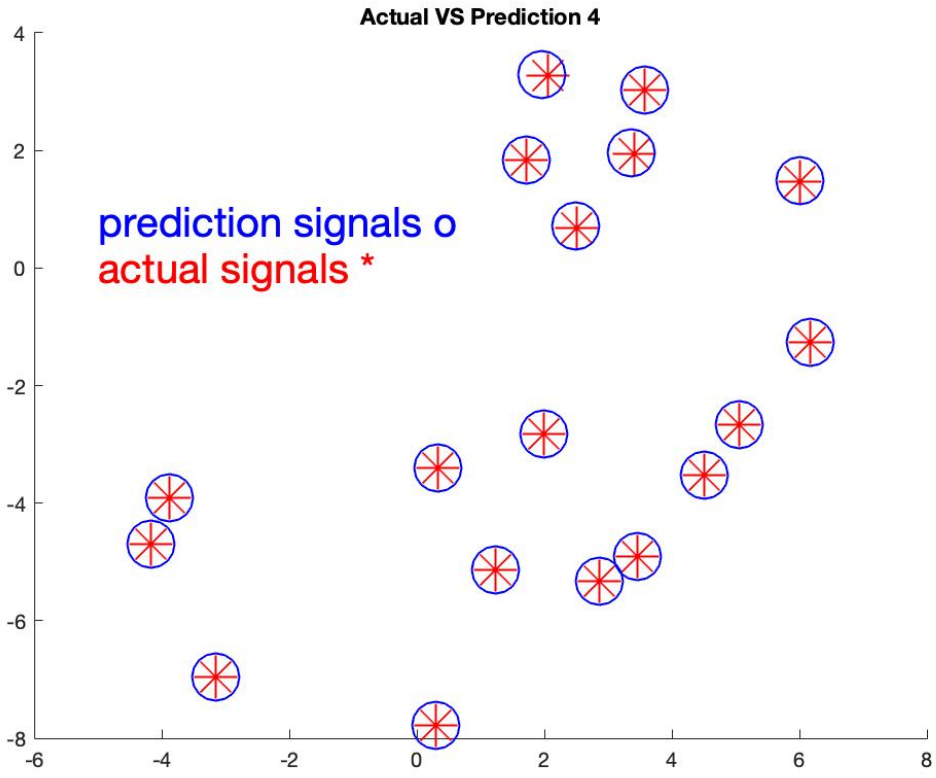

Figure 3.4: Fourth Group: prediction values VS Actual output

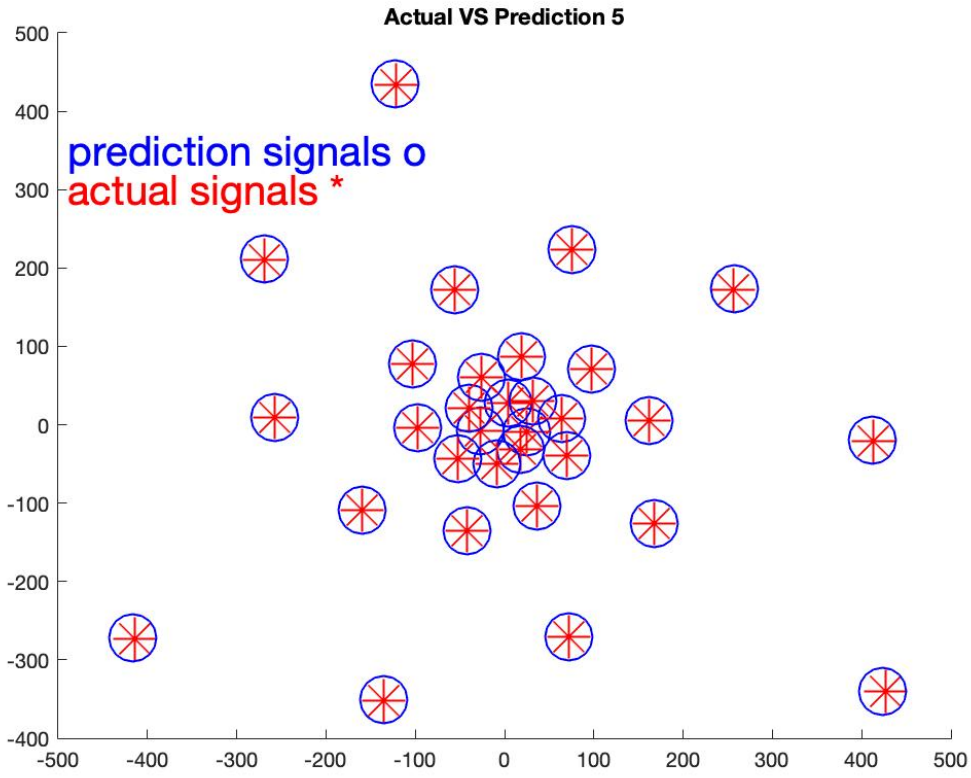

Figure 3.5: Fifth Group: prediction values VS Actual output

Chapter 4

Co-prime Sampling

This chapter proposes a theory of co-prime sampling to efficiently determine the original poles and residues of the sum signal. We used features of the sum signal and the linear Diophantine equation to prove the theory. We will first introduce co-prime sampling, followed by a detailed proof of this theory in the second section. After that, we will provide simulation data sets and their implementations of the co-prime sampling. Before implementations, our generated simulation data needs to utilize the alternative method of Padé approximation to find Hankel matrices' generalized eigenvalues.

4.1 Theory Of Co-prime Sampling

One of our main technical contributions in this thesis is the following theorem:

Theorem 1. *Let p and q are co-prime each other, and let $c_1 = |c_| \exp(\arg(c_1))$ and $c_2 = |c_2| \exp(\arg(c_2))$ be two complex numbers. Then, a pair of polynomial equations $z^p = c_1$ and $z^q = c_2$ has a solution with respect to a complex variable z if and only if*

the following two conditions must be met simultaneously:

1. *The magnitudes of c_i must satisfy $|c_1|^{1/p} = |c_2|^{1/q}$.*

2. *The phases of c_i must satisfy a) $\frac{\arg(c_1)q - \arg(c_2)p}{2\pi}$ is an integer, and b) there exist two integers m_p and n_q: $0 \leq m_p < q$ and $0 \leq n_q < p$, such that $\frac{\arg(c_1)q - \arg(c_2)p}{2\pi} = m_p p - n_q q$.*

Furthermore, under the above two conditions, the solution of a set of equations: $z^p = c_1$ and $z^q = c_2$ is unique, and can be explicitly determined by

$$\begin{aligned} m_p &= k\bar{p} + q\left\lceil -\frac{k\bar{p}}{q} \right\rceil \\ n_q &= \frac{p\bar{p}-1}{q}k + p\left\lceil -\frac{k\bar{p}}{q} \right\rceil \end{aligned}$$

where $k = \frac{\arg(c_1)q - \arg(c_2)p}{2\pi}$. ■

4.2 Proof Of The Theory

In order to prove this theorem, we need to establish the following two lemmas.

Lemma 1. *If $\gcd(p, q) = 1$, the Diophantine equation $pm + qn = k$ has integer solutions with respect to variables m and n. Furthermore, all sets of solutions can be characterized by $m = \bar{p}k + qt, \quad n = \frac{1-p\bar{p}}{q}k - pt$, where t is any integer and $\bar{p}$ is such an integer that $1 \leq \bar{p} < q$ and $p\bar{p} \equiv 1 \mod q$.* ■

Proof: From (Hua, 1982) we know that the Diophantine equation $pm + qn = k$ with respect to integer variables m and n indeed has integer solutions. Now we only need to characterize all the solutions. To do that, consider the corresponding

congruent equations: $pm \equiv k \mod q$. Since $\gcd(p,q) = 1$, this congruent equation has a unique solutions, $m = \bar{p}k \mod q$, where $p\bar{p} \equiv 1 \mod q$. Hence, all the solutions can be represented by $m = \bar{p}k + qt$, where t is an arbitrary integer. Now, substituting this m into $pm + qn = k$ yields $n = \frac{1-p\bar{p}}{q}k - pt$, as required. This completes the proof of Lemma 1. □

Lemma 2. *Let two positive integers p and q be coprime. Then, for any given integer k, there exists a unique pair of integers m and n such that $k = pm+qn$ for $0 \le m < q$, which is explicitly determined by $m = k\bar{p} + q\left\lceil -\frac{k\bar{p}}{q} \right\rceil$ and $n = \frac{1-p\bar{p}}{q}k - p\left\lceil -\frac{k\bar{p}}{q} \right\rceil$.* ■

We are now in a position to prove Theorem 1.

Proof of Theorem 1: By Lemma 1, we know that all the solutions to $k = pm + qn$ are given by $m = \bar{p}k + qt$ and $n = \frac{1-p\bar{p}}{q}k - pt$. Now, we only need to prove that under the constraint $0 \le m < q$, there exists only one t. To this end, we enforce $m = \bar{p}k + qt$ to satisfy this constraint, i.e.,

$$0 \le \bar{p}k + qt < q$$

which is equivalent to $-\frac{\bar{p}k}{q} \le t < 1 - \frac{\bar{p}k}{q}$. Within this interval, there is one and only one integer $t = \left\lceil -\frac{k\bar{p}}{q} \right\rceil$. Hence, we have a unique pair of $m = k\bar{p} + q\left\lceil -\frac{k\bar{p}}{q} \right\rceil$ and $n = \frac{1-p\bar{p}}{q}k - p\left\lceil -\frac{k\bar{p}}{q} \right\rceil$. This comeplets the proof of Lemma 2. □

Proof: Let $z = |z|e^{j\theta}$ with $0 \le \theta < 2\pi$. Then, a system of equations: $z^p = c_1$ and $z^q = c_2$, has a solution if and only if $|z| = |c_1|^{1/p} = |c_2|^{1/q}$ and there exist two integers m_p and n_q such that

$$p\theta = \arg(c_1) + 2n_q\pi \text{ and } q\theta = \arg(c_2) + 2m_p\pi \tag{4.2.1}$$

Since $0 \leq \theta, \arg(c_k) < 2\pi$, we have $0 \leq m_p < q$ and $0 \leq n_q < p$. Note that a set of equations (4.2.1) is equivalent to the following fact that 1) $\frac{\arg(c_1)q - \arg(c_2)p}{2\pi}$ is an integer, and 2) there exist two integers m_p and n_q: $0 \leq m_p < q$ and $0 \leq n_q < p$, such that

$$\frac{\arg(c_1)q - \arg(c_2)p}{2\pi} = m_p p - n_q q \tag{4.2.2}$$

Suppose now that $\frac{\arg(c_1)q - \arg(c_2)p}{2\pi}$ is an integer, and that a system of equations (4.2.2) has a solution. Now, by Lemma 2, we have a unique pair of solution, given by

$$\begin{aligned} m_p &= k\bar{p} + q\left\lceil -\frac{k\bar{p}}{q} \right\rceil \\ n_q &= \frac{p\bar{p} - 1}{q}k + p\left\lceil -\frac{k\bar{p}}{q} \right\rceil \end{aligned}$$

where $k = \frac{\arg(c_1)q - \arg(c_2)p}{2\pi}$. This completes the proof of Theorem 1. □

4.3 Simulation Data Sets And their Implementations

This section will show several simulation data algorithms, followed by implementations of those generated data sets in Co-prime sampling. Results will be demonstrated in both data and figures

First of all, there are two groups of data x which can be created by the formula

$$x_n(t) = e^{\sqrt{2}\pi it} + e^{\sqrt{3}\pi it} + e^{\sqrt{5}\pi it} + e^{\sqrt{6}\pi it} + e^{\sqrt{7}\pi it}$$

where the first group of data is produced when $t = 3nT$, and the other group is when $t = 2nT$. Since $2 \times \sqrt{7}\pi \leq \frac{2\pi}{T}$, we can get $T \leq \frac{1}{3}$. Base on the number of entries in $x_n(t)$, in order to find the two groups of corresponding generalized eigenvalues of two Hankel matrices, similarly to the forms of (2.3.1) and (2.3.2), which are formed by these 2 data sets, the size of data need to double of the size of eigenvalues, where

$$n = 0, 1, 2, \ldots 9$$

.

Data Index	**x(t = 3nT)**	**x(t = 2nT)**
0	$5.000 + 0.000i$	$5.000 + 0.000i$
1	$-2.618 + 3.592i$	$0.503 + 4.722i$
2	$-0.754 - 2.878i$	$-3.955 + 0.801i$
3	$0.853 + 0.850i$	$-0.754 - 2.878i$
4	$-0.082 - 1.205i$	$1.730 - 0.332i$
5	$1.397 + 1.709i$	$-0.381 + 0.744i$
6	$-2.443 + 0.035i$	$-0.082 - 1.205i$
7	$1.109 - 1.571i$	$1.930 + 0.203i$
8	$0.296 + 0.978i$	$-0.173 + 2.375i$
9	$-0.179 - 0.178i$	$-2.443 + 0.035i$

As mentioned in the previous section (2.3.1), we can form a Hankel matrix and a shifted Hankel matrix for each data set. As the result, we can eventually get 2 groups of generalized eigenvalues respectively, which are individually in a size of 5. The groups of sorted eigenvalues from minimal phases to maximum phases are

Eigenvalues Index	**E(t = 3nT)**	**E(t = 2nT)**
0	$e^{1.481i}$	$e^{0.987i}$
1	$e^{1.814i}$	$e^{1.209i}$
2	$e^{2.342i}$	$e^{1.561i}$
3	$e^{2.565i}$	$e^{1.710i}$
4	$e^{2.771i}$	$e^{1.847i}$

The common aspect of those Eigenvalues is that their magnitudes are 1. In other words, the eigenvalues will scatter along the circle whose center is at coordinate $(0, 0)$ with radius 1. These two groups of eigenvalues show in the *Figure* 4.1 and *Figure* 4.2 at the end of this chapter.

Since the magnitudes of those eigenvalues are approximately equal to 1, each group of eigenvalues is sorted based on their phase values from smallest to largest. The corresponding eigenvalues of 2 groups with the same index can be apply to co-prime theory as c_1 and c_2. Firstly, using the phases of c_1 and c_2, and two random pre-defined co-prime values of p and q (4.2.2) , m_p and n_q can be determined. Since

the magnitudes of c_1 and c_2 are always 1, the first condition of theorem1 is already satisfied. As for condition 2, using the existing values of q equals 2, and p equals 3. For the phases of eigenvalues, we can get an integer value k. The values m_p and n_q are determined from the previous step are proved to be integers, and satisfy the limits that $0 \leq m_p < q$ and $0 \leq n_q < p$. Since the two conditions of co-prime theory meet simultaneously, we can find the only value of θ. Therefore, we can find the one and the only z value for each corresponding θ, which leads to 5 z values in general. The distribution of z shows in $figure$4.3

Besides, it can prove that the five angles, θ values gained from the implementation of co-prime theory are the same as five ω values based on the algorithm of simulation $x_n(t)$, which show in the table:

ω_1	ω_2	ω_3	ω_4	ω_5
$\sqrt{2}\pi T$	$\sqrt{3}\pi T$	$\sqrt{5}\pi T$	$\sqrt{6}\pi T$	$\sqrt{7}\pi T$

On the other hand, If we change from $t = 3nT$ and $t = 2nT$ to $t = 5nT$ and $t = 3nT$, and give value $T = 1/25$ based on its limit, we can generate the other 2 new groups of data whose magnitudes are still equal to one. The data sets generated based on the previous formula can be

Data Index	**x(t = 5nT)**	**x(t = 3nT)**
0	$5.000 + 0.000i$	$5.000 + 0.000i$
1	$1.200 + 4.644i$	$3.466 + 3.500i$
2	$-3.701 + 2.009i$	$-0.054 + 4.707i$
3	$-2.182 - 2.502i$	$-3.146 + 3.012i$

Continued on the next page

Continued from previous page

Data Index	**x(t = 5nT)**	**x(t = 3nT)**
4	$1.446 - 1.721i$	$-3.882 - 0.151i$
5	$0.853 + 0.850i$	$-2.182 - 2.502i$
6	$-0.829 - 0.065i$	$0.319 - 2.669i$
7	$0.692 - 1.266i$	$1.705 - 1.097i$
8	$1.879 + 0.840i$	$1.277 + 0.556i$
9	$-0. + 2.345i$	$-0.074 + 0.903i$

Similarly, we can get the following 2 groups of generalized eigenvalues with magnitudes 1,

Eigenvalues Index	**E(t = 5nT)**	**E(t = 3nT)**
0	$e^{0.889i}$	$e^{0.533i}$
1	$e^{1.088i}$	$e^{0.653i}$
2	$e^{1.405i}$	$e^{0.843i}$
3	$e^{1.539i}$	$e^{0.923i}$
4	$e^{1.662i}$	$e^{0.997i}$

Apply the above 2 groups of simulation data into the co-prime theory. As you can see, all the conditions met the same as the previous implementation except that $q = 3$

and $p = 5$, we can have the same results as the former implementation.

Along with this, we have added coefficients to upgraded the algorithm of simulation data, and extend the terms of algorithm. The algorithm is $x_n(t) = 3.2e^{\sqrt{2}\pi it} + 3.7e^{\sqrt{3}\pi it} + 5.2e^{\sqrt{5}\pi it} + 6.3e^{\sqrt{6}\pi it} + 7.1e^{\sqrt{7}\pi it} + 1.3e^{\sqrt{11}\pi it} + 1.11e^{\sqrt{2.71}\pi it} + 9.13e^{\sqrt{3.91}\pi it} + 4.73e^{\sqrt{11.7}\pi it} + e^{\sqrt{7.57}\pi it}$. In this case, the restriction of T is still $T \leq \frac{1}{3}$. In contrast to the former simulation data sets, I generate 2 groups of data with $t = 3nT$ and $t = 2nT$, and choose $T = 1/11$. The simulation data sets are

Data Index	**x(t = 9nT)**	**x(t = 7nT)**
0	$42.800 + 0.000i$	$42.800 + 0.000i$
1	$-15.60 + 34.70i$	$0.731 + 39.840i$
2	$-18.944 - 18.60i$	$-32.04 + 2.086i$
3	$12.040 - 9.122i$	$-4.200 - 21.930i$
4	$6.543 + 7.472i$	$12.590 - 6.520i$
5	$-7.337 + 2.550i$	$7.971 + 6.390i$
6	$4.715 - 3.812i$	$-4.112 + 7.503i$
7	$5.412 + 6.373i$	$-4.653 - 4.781i$
8	$2.174 - 10.510i$	$6.273 + 0.097i$
9	$3.456 + 11.518i$	$-5.412 + 6.373i$
10	$-10.150 - 8.876i$	$-3.822 - 9.617i$
11	$13.292 - 0.535i$	$11.407 + 1.138i$
12	$-4.911 + 7.836i$	$-6.923 + 10.424i$
13	$-2.982 - 1.657i$	$-7.421 - 11.400i$
14	$-2.152 - 4.720i$	$12.871 - 3.913i$

Continued on the next page

Continued from previous page

Data Index	**x(t = 9nT)**	**x(t = 7nT)**
15	$6.870 + 0.010i$	$1.488 + 10.900i$
16	$-3.350 + 2.801i$	$-6.437 + 1.072i$
17	$2.852 - 0.290i$	$-2.521 - 1.423i$
18	$-5.490 + 1.303i$	$-2.152 - 4.719i$
19	$5.927 - 4.001i$	$6.147 - 3.114i$

Thus, we can have the following generalized Eigenvalues of 2 Hankel matrices

Eigenvalues Index	**E(t = 9nT)**	**E(t = 7nT)**
0	$e^{2.931i}$	$e^{2.280i}$
1	$e^{2.840i}$	$e^{2.210i}$
2	$e^{2.357i}$	$e^{1.801i}$
3	$e^{2.267i}$	$e^{1.733i}$
4	$e^{2.098i}$	$e^{1.592i}$
5	$e^{1.915i}$	$e^{1.533i}$
6	$e^{1.211i}$	$e^{1.319i}$
7	$e^{1.694i}$	$e^{0.942i}$
8	$e^{1.484i}$	$e^{1.142i}$
9	$e^{1.410i}$	$e^{1.062i}$

As you can see from the table, the magnitudes of those generalized eigenvalues are equal to 1. The distribution figures are shown in $Figure4.4$ and $Figure4.5$.

As a sequence of implementation, accompanying the condition $q = 7$, $p = 9$, will result in ten θ solutions equal to $\sqrt{2}\pi T$, $\sqrt{2.71}\pi T$, $\sqrt{3}\pi T$, $\sqrt{3.91}\pi T$, $\sqrt{5}\pi T$, $\sqrt{6}\pi T$, $\sqrt{7}\pi T$, $\sqrt{7.57}\pi T$, $\sqrt{11}\pi T$, $\sqrt{11.7}\pi T$, respectively. Since the magnitudes of z equal to 1, all the z will locate on the unit circle, which is found on $figure4.6$

Similarly, we extend our simulation data set to a size of 60. For the fourth data group, we set $T = 1/13$, the first group of data is $X(t = 9nt)$, and the second group is $X(t = 7nt)$. The data sets can form four Hankel matrices, resulting in two groups of the size of 30 generalized eigenvalues. The distribution Figures are $Figure4.7$ and $Figure4.8$. Moreover, the $figure4.9$ is for the solution z of this simulation set.

Subsequently, we generate another algorithm to produce simulation data, which is

$$x_n(t) = e^{\frac{\pi}{3}ti} + e^{\frac{\pi}{5}ti} + e^{\frac{\pi}{7}ti} + e^{\frac{\pi}{11}ti} + e^{\frac{\pi}{13}ti} + e^{\frac{\pi}{17}ti}$$

The limit of T changes to $T \leq 3$ Since the algorithm has 6 entries. Thus, we need to generate each group of data that double this size. Therefore, the index is

$$i = 0, 1, 2, 3, \ldots 11$$

We also set that $T = 1/2$, the first group with $t = 10nT$ and the second group with $t = 3nT$

Data Index	**x(t = 10nT)**	**x(t = 3nT)**
0	$6.000 + 0.000i$	$6.000 + 0.000i$
1	$2.042 + 4.070i$	$4.176 + 3.476i$
2	$-0.024 + 2.639i$	$1.167 + 3.871i$
3	$-1.571 + 2.573i$	$0.035 + 2.794i$
4	$-1.704 + 0.066i$	$-0.286 + 2.724i$
5	$-0.928 + 1.321i$	$-1.571 + 2.573i$
6	$-3.332 - 0.579i$	$-2.316 + 0.990i$
7	$-0.313 - 2.437i$	$-1.223 - 0.048i$
8	$-0.289 - 0.760i$	$-0.601 + 0.925i$
9	$0.345 - 2.080i$	$-2.159 + 1.414i$
10	$1.256 - 0.588i$	$-3.332 - 0.579i$
11	$1.405 - 1.300i$	$-1.813 - 2.564i$

These 2 groups of data lead to 2 groups of Hankel matrices, followed by the same size of generalized eigenvalues independently, which are sorted as

Eigenvalues Index	**E(t = 10nT)**	**E(t = 3nT)**
0	$e^{0.462i}$	$e^{0.277i}$
1	$e^{0.604i}$	$e^{0.362i}$
2	$e^{0.714i}$	$e^{0.428i}$

Continued on the next page

Continued from previous page

Eigenvalues Index	**E(t = 10nT)**	**E(t = 3nT)**
3	$e^{1.122i}$	$e^{0.673i}$
4	$e^{1.571i}$	$e^{0.942i}$
5	$e^{2,618i}$	$e^{1.571i}$

It is redoubtable that the magnitudes of eigenvalues equal to 1. Therefore we use those eigenvalues to implement into the co-prime theory, with the settings that $q = 3$ and $p = 10$. The results of implementation are revealed by the values of θ. Where θ equal to the ω from the entries of the simulation algorithm. Be more specific that they are equal to the exponent of each exponential part.

ω_1	ω_2	ω_3	ω_4	ω_5	ω_5
$\frac{\pi T}{17}$	$\frac{\pi T}{13}$	$\frac{\pi T}{11}$	$\frac{\pi T}{7}$	$\frac{\pi T}{5}$	$\frac{\pi T}{3}$

Based on the prior simulation formula, if we only change the values of t that $t = 3nT$ for the first group of dataset and $t = 2nT$ for the second group, we will get the simulation data

Data Index	**X(t = 3nT)**	**X(t = 2nT)**
0	$6.000 + 0.000i$	$6.000 + 0.000i$
1	$4.176 + 3.476i$	$5.123 + 2.592i$
2	$1.167 + 3.871i$	$3.092 + 3.966i$
3	$0.035 + 2.794i$	$1.167 + 3.871i$
4	$-0.286 + 2.724i$	$0.191 + 3.103i$
5	$-1.571 + 2.573i$	$-0.024 + 2.639i$
6	$-2.316 + 0.990i$	$-0.286 + 2.724i$
7	$-1.223 - 0.048i$	$-1.071 + 2.779i$
8	$-0.601 + 0.925i$	$-2.009 + 2.168i$
9	$-2.159 + 1.414i$	$-2.316 + 0.990i$
10	$-3.332 - 0.579i$	$-1.704 + 0.066i$
11	$-1.813 - 2.564i$	$-0.800 + 0.107i$

As a result of the 2 simulation data groups, two groups of generalized Eigenvalues which distribute along the circle of radius 1 will form

Eigenvalues Index	**E(t = 3nT)**	**E(t = 2nT)**
0	$e^{0.277i}$	$e^{0.185i}$
1	$e^{0.362i}$	$e^{0.242i}$
2	$e^{0.428i}$	$e^{0.286i}$

Continued on the next page

Continued from previous page

Eigenvalues Index	**E(t = 3nT)**	**E(t = 2nT)**
3	$e^{0.673i}$	$e^{0.449i}$
4	$e^{0.942i}$	$e^{0.628i}$
5	$e^{1.571i}$	$e^{1.047i}$

Indeed, after implementing the above data sets, the outcome will be identified as the former implementation.

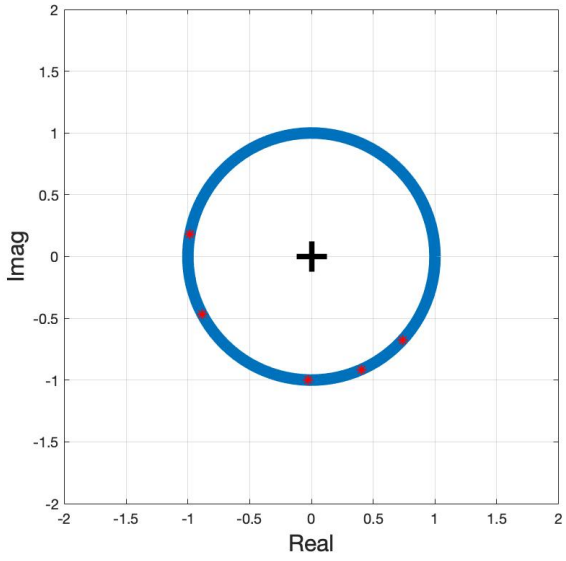

Figure 4.1: First simulation group: Distribution of generalized eigenvalues $\mathbf{E(t = 3nT)}$

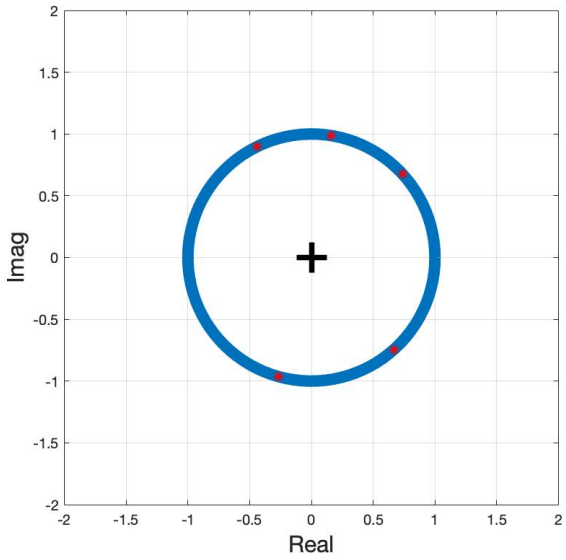

Figure 4.2: First simulation group: Distribution of generalized eigenvalues $\mathbf{E(t = 2nT)}$

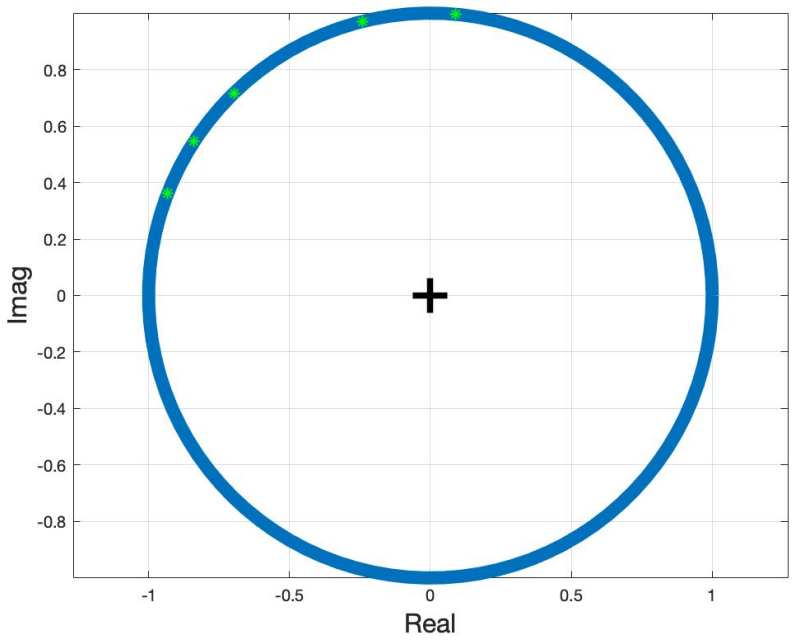

Figure 4.3: z of the first data set

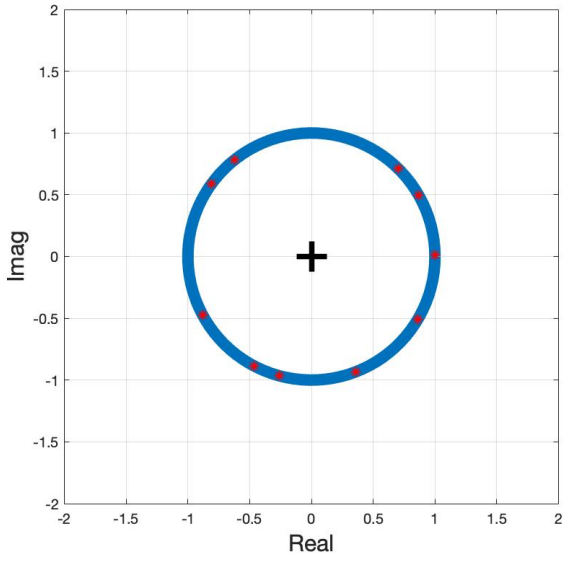

Figure 4.4: Second simulation group: Distribution of generalized eigenvalues $\mathbf{E(t = 11nT)}$

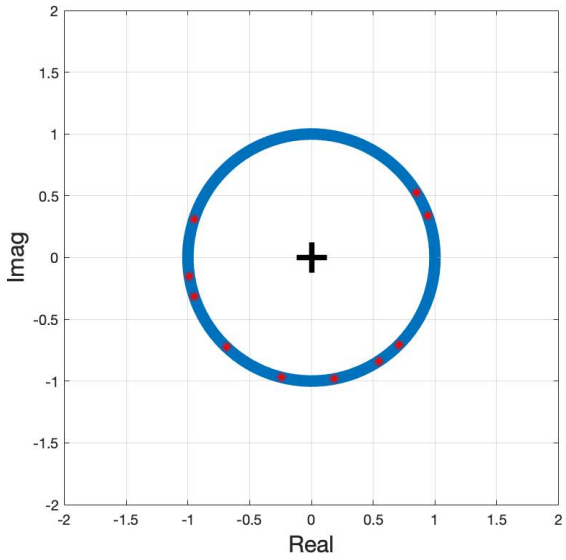

Figure 4.5: Second simulation group: Distribution of generalized eigenvalues $\mathbf{E(t = 9nT)}$

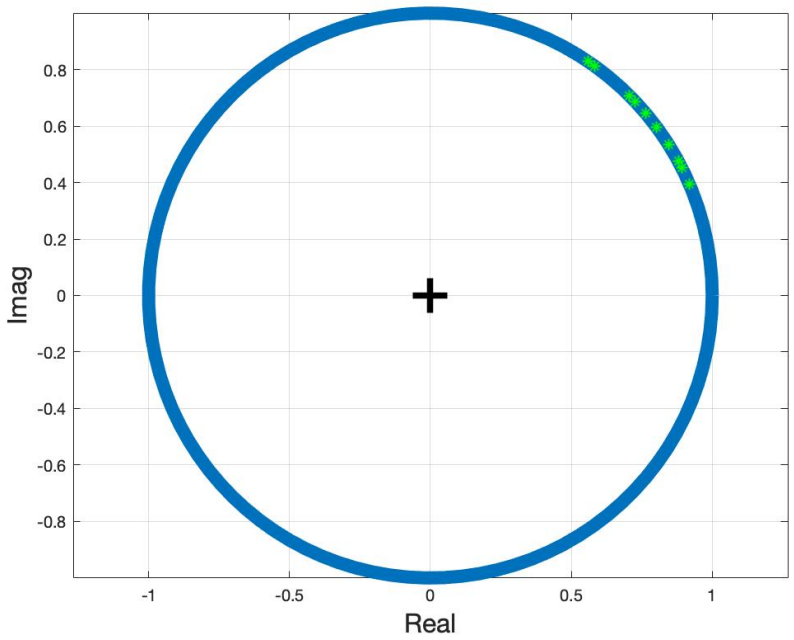

Figure 4.6: z of the second data set

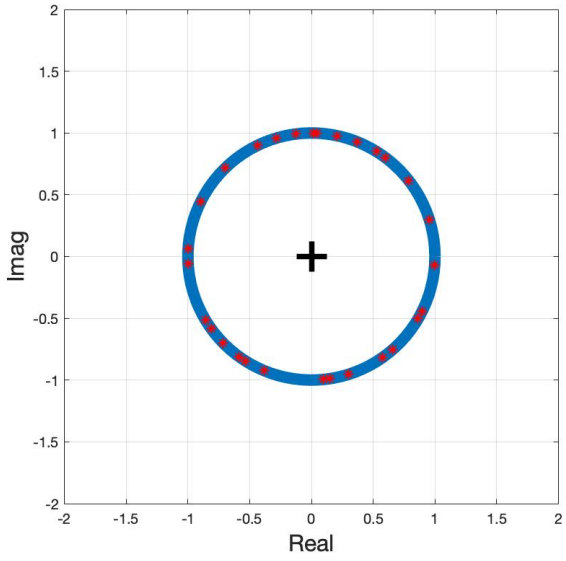

Figure 4.7: Third simulation group: Distribution of generalized eigenvalues $\mathbf{E(t = 7nT)}$

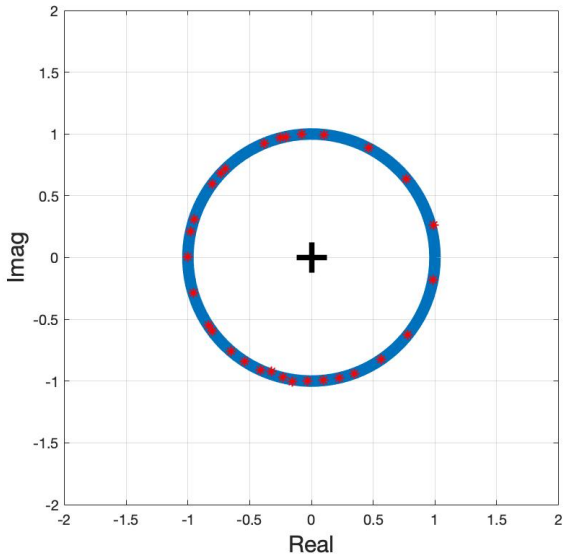

Figure 4.8: Third simulation group: Distribution of generalized eigenvalues $\mathbf{E(t = 9nT)}$

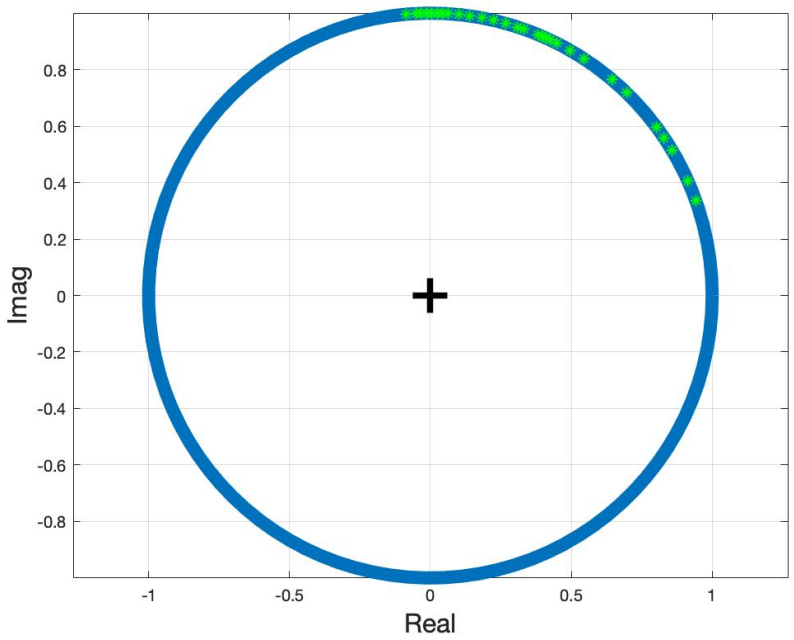

Figure 4.9: z of the third data set

Chapter 5

Conclusion and Future Work

In this thesis, we have demonstrated several traditional ways of Padé approximation, especially the SVD-based approach of approximation that deals with an exact degree. Its alternative method that uses generalized Hankel Eigenvalues to find the poles of Padé approximants. Other than that, the primary purpose of this paper is to propose a data prediction method that is built based on the features of Padé approximation. How reliable can this data prediction method be? After proposing this data prediction model, we display our algorithms to generate simulation data and implement those data into our prediction model in stages. At the end of implementation, comparisons between simulation output data and the prediction outcomes are duplicate without any error. The results denote our proposed data prediction model's accuracy when in terms of simulation data.

Besides the proposed data prediction model, we also prove the theory of co-prime sampling with the utilization of padé approximation's extracted features. In the same way as chapter 3, we provide detailed proof for this theory and additional evidence with simulation data groups. Notably, outcomes of all the simulation data groups'

implementations can prove this theory by using the Generalized Eigenvalues of Hankel matrices.

Our proposed data prediction method works precisely with simulation data while more efforts are required. The first aspect is the data noise. Currently, our simulation data has not included noise yet. However, to make our proposed data prediction method applicable, improving the model with noisy data is inescapable. In the future, our first step is to improve by training our data prediction model with simulation data, which contains random noise and find the correct regularization to minimize the error. Afterward, we can consider collecting real-world data in different fields and using those data to train our proposed model, accompanying them to make adjustments for our algorithms in different fields to get the best prediction results. This future work also applies to the co-prime theory.

Our goal is to make our prediction model accurate and efficient, which can be applicable in a variety of fields. For instance, in the financial field, if a mobile devices' application developed originally from our proposed prediction method would be used by individual investors who could easily monitor their investments on their mobile devices anytime. Companies' strategists who were lack of data to make a decision would use this application to predict some related data as convincing evidence, or traders who might not be dependable on this application, but they could use it as an alert before trading the stocks. Similarly, in the electrical field, the communication system can use it to predict more signal data; in the health industry, it can be implemented into health monitor equipment to help with doctors' diagnosis to look for reliable data that might be the blind point for the equipment. Other possible fields of application of our proposed method might suffer due to lack of data, such as data

analyst when they are lack of analysis data they will need to predict more. When people were lack of data, they could use the current data with Padé approximation to extract the data features and use data prediction(3.1.5)to gain more reliable statistics that can overcome the problem.

Bibliography

B. Beckermann, G. H. G. and Labahn, G. (2007). On the numerical condition of a generalized hankel eigenvalue problem. *Numerische Mathematik*, **145**(106), 41–68.

Beckermann, B. (2000). The condition number of real vandermonde, krylov and positive definite hankel matrices. *Numerische Mathematik*, **145**(85), 553–577.

Belkic, D. and Belkic, K. (2006). In vivo magnetic resonance spectroscopy by the fast padé transform. *Physics in medicine and biology*, **51**(5), 1049–1076.

Böttcher, A. and Grudsky, S. M. (2005). *Spectral Properties of Banded Toeplitz Matrices*. Society for Industrial and Applied Mathematics.

Froissart, M. (1969). Approximation de pade application à la physique des particules élémentaires. *RCP, Programme No. 25*, **9**(2), 1–13.

G. A. Baker, J. and Graves-Morris, P. R. (1996). *Padé approximants*. Cambridge University Press.

Gene H. Golub, P. M. and Varah, J. (1999). A stable numerical method for inverting shape from moments. *SIAM J. Sci. Comput.*, **21**(4), 1222–1243.

Gilewicz, J. and Pindor, M. (1997). Padé approximants and noise: a case of geometric series. *Journal of Computational and Applied Mathematics*, **87**(2), 199–214.

Hua, L.-K. (1982). *Introduction to Number Theory*. Springer-Verlag Berlin Heidelberg.

Hunaidi, O. and Chu, W. T. (1999). Acoustical characteristics of leak signals in plastic water distribution pipes. *Applied Acoustics*, **58**(3), 235–254.

Junior, L. S. and Franca, I. D. P. (2011). Shocks in financial markets, price expectation, and damped harmonic oscillators. *General Finance (q-fin.GN)*.

Mark Giesbrecht, G. L. and shin Lee, W. (2009). Symbolic–numeric sparse interpolation of multivariate polynomials. *Journal of Symbolic Computation*, **44**(8), 943–959.

Mazza, M. and Pestana, J. (2019). Spectral properties of flipped toeplitz matrices and related preconditioning. *BIT Numerical Mathematics*, **60**(59), 463–482.

Nicholas Daras, V. N. (2011). Universal padé approximation. visited on 2020-02-20.

Pedro Gonnet, R. P. and Trefethen, L. N. (2011). Robust rational interpolation and least-squares. *Electronic Transactions on Numerical Analysi*, **38**, 146–.

Pedro Gonnet, S. G. and Trefethen, L. N. (2018). Robust pade approximation via svd. *The Quarterly Journal of Mechanics and Applied Mathematics*, **73**(1), 36–50.

Perotti, L. and Wojtylak, M. (2018). Matrix methods for pade approximation: numerical calculation of poles, zeros and residues.

Robert M. Corless, Patrizia M. Gianni, B. M. T. and Watt, S. M. (1995). The singular value decomposition for polynomial systems. *Proceedings of the 1995 international symposium on Symbolic and algebraic computation*, pages 195–207.

Szabo, F. E. (2015). *The Linear Algebra Survival Guide*. Academic Press.

Wu, M.-C. (2014). Damped oscillatory behaviors in the ratios of stock market indices. *Proceedings of the International Conference on Social Modeling and Simulation, plus Econophysics Colloquium 2014*, pages 51–62.